Functional Reconstitution of the Integral Membrane Enzyme, Isoprenylcysteine Carboxyl Methyltransferase, in Synthetic Bolalipid Membrane Vesicles[†]

Wilma Febo-Ayala, Shakira L. Morera-Félix, Christine A. Hrycyna,* and David H. Thompson*

Department of Chemistry, Purdue University, 560 Oval Drive, West Lafayette, Indiana 47907-2084

Received June 10, 2006; Revised Manuscript Received September 15, 2006

ABSTRACT: Three bipolar archaeal-type diglycerophosphocholine tetraether lipids (also known as bolalipids) have been prepared to determine (1) the influence of molecular structure on the physical properties of bolalipid membranes and (2) their impact on the functional reconstitution of Ste14p, a membrane-associated isoprenylcysteine carboxyl methyltransferase from *Saccharomyces cerevisiae*. Three bolalipids were synthesized: $C_{20}BAS$, $C_{32}BAS$, and $C_{32}phytBAS$. These bolalipid structures differ in that the $C_{20}BAS$ derivative has a short *sn*-1 glyceryl diether $C_{20}H_{40}$ transmembrane alkyl chain and two ether-linked *sn*-2 *n*-decyl chains, whereas the $C_{32}BAS$ and $C_{32}phytBAS$ derivatives have a longer *sn*-1 diether $C_{32}H_{64}$ membrane-spanning chain and two ether-linked *sn*-2 *n*-hexadecyl or phytanyl chains, respectively. Differential scanning calorimetry and temperature-dependent ^{31}P NMR was used to determine the gel-to-liquid crystalline phase transition temperatures of the bolalipids ($C_{32}BAS$ $T_m > 85$ °C; $C_{32}phytBAS$ $T_m = 14$ °C; and $C_{20}BAS$ $T_m = 17$ °C). The bolalipid lateral diffusion coefficients, determined by fluorescence recovery after photobleaching at 25 °C, were 1.5×10^{-8} and 1.8×10^{-9} cm²/s for $C_{20}BAS$ and C_{32}-phytBAS, respectively. The mobility of $C_{32}BAS$ could not be measured at this temperature. Ste14p activity was monitored by an *in vitro* methyltransferase assay in reconstituted vesicle dispersions composed of DMPC, $C_{20}BAS$/*E. coli* polar lipid, $C_{20}BAS$/POPC, $C_{32}phytBAS$/*E. coli* polar lipid, and $C_{32}phytBAS$/POPC. Ste14p activity was lost in vesicles composed of 75−100 mol % $C_{20}BAS$ and 0−100 mol % $C_{32}BAS$ but retained in vesicles with 0−50 mol % $C_{20}BAS$ and 0−100 mol % $C_{32}phytBAS$. Confocal immunofluorescence microscopy confirmed the presence of Ste14p in 100 mol % $C_{20}BAS$ and 100 mol % $C_{32}phytBAS$ vesicle dispersions, even though the lamellar liquid crystalline phase thickness of C_{20}-BAS is only 32 Å. Because Ste14p activity was not affected by either the gel-to-liquid-crystal phase transition temperature of the lipid or the temperature of the assay, the low activity observed in 75−100 mol % $C_{20}BAS$ membranes can be attributed to hydrophobic mismatch between this bolalipid and the hydrophobic surface of Ste14p.

Bolalipids, also called bolaamphiphiles, are a class of bipolar lipids found in the cell membranes of some *Archaea*. In many cases, these organisms can survive in extreme environments because of the presence of isoprenoid-based tetraether bolalipids in their membranes (*1−5*). The membrane-spanning bipolar structural motif confers increased stability to these membranes by effectively cross-linking the apposed leaflets of a bilayer membrane, thereby producing a mono-layer membrane that functionally mimics a conventional membrane bilayer. This membrane stabilization strategy blocks membrane failure via delamination in the physically and chemically challenging environments that are often preferred by this class of organisms. Archaeal bolalipid structures are characterized by ether linkages to each glycerol backbone, phosphate or sugar polar headgroups, and trans-

membrane chains that contain combinations of methyl branching and cyclopentane rings to help maintain membrane fluidity across a wide range of environmental temperatures (*6−7*). Studies of biogenic and synthetic variants of these unusual membrane materials demonstrate that bolalipid membranes are less permeable and more durable than membranes composed of monopolar lipids (*8−13*). This unique combination of properties has ignited interest in their

---

* To whom correspondence should be addressed. Phone: 765-494-7322. Fax: 765-496-2592. E-mail: hrycyna@purdue.edu (C.A.H.). Phone: 765-494-0386. Fax: 765-496-2592. E-mail: davethom@purdue.edu (D.H.T.).

[1] Abbreviations: AFC, *N*-acetyl-*S*-farnesyl-L-cysteine; ^{14}C-SAM, *S*-adenosyl-L-[^{14}C-methyl] methionine; $C_{20}BAS$, 2,2′-di-*O*-decyl-3,3′-di-*O*-(1″,20″-eicosanyl)-bis-(*rac*-glycero)-1,1′-diphosphocholine; C_{32}-BAS, 2,2′-di-*O*-hexadecyl-3,3′-di-*O*-(1″,32″-dotriacontanyl)-bis-(*rac*-glycero)-1,1′-diphosphocholine; $C_{32}phytBAS$, 2,2′-di-*O*-(3,7,11,15-tetramethylhexadecyl)-3,3′-di-*O*-(1″,32″-dotriacontanyl)-bis-(*rac*-glycero)-1,1′-diphosphocholine; Chol, cholesterol; DDM, 1-dodecyl-*β*-D-maltopyranoside; DMF, *N,N*-dimethylformamide; DMPC, 1,2-dimyristoyl-*sn*-glycero-3-phosphocholine; DSC, differential scanning calorimetry; *E. coli* polar lipid, commercial polar lipid extract from *E. coli*; FRAP, fluorescence recovery after photobleaching; Ste14p, His$_{10}$myc$_3$-tagged Ste14p Icmt isolated from *S. cerevisiae*; Icmt, isoprenylcysteine carboxyl methyltransferase; NBD-OPPC, 1-oleoyl-2-[6-[(7-nitro-2-1,3-benzoxadiazol-4-yl)amino]hexanoyl]-*sn*-glycero-3-phosphocholine; POPC, 1-palmitoyl-2-oleoyl-*sn*-glycero-3-phosphocholine; SDS, sodium dode-cylsulfate; THF, tetrahydrofuran; Tris, tris(hydroxymethyl)aminomethane.
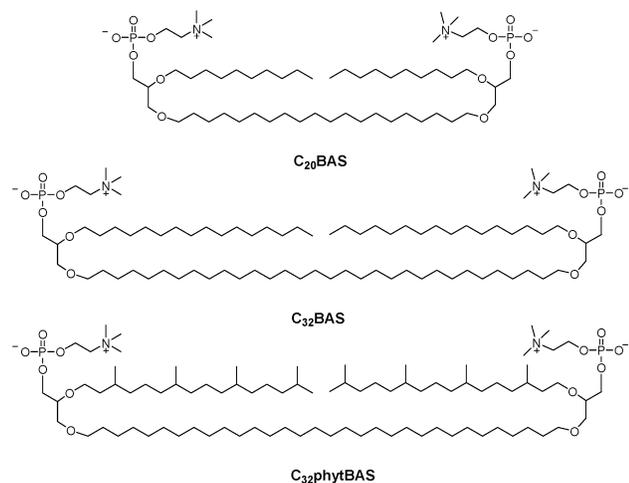
FIGURE 1: Structures of the synthetic bolalipids used in this study: $C_{20}BAS$, $C_{32}BAS$, and $C_{32}phytBAS$.

use as nonpolymeric membrane stabilizing agents in applications such as drug delivery and membrane-protein-based biosensors (*5, 12, 14, 15*).

Biosensor and drug delivery applications of bolalipids will require large quantities of material. Unfortunately, bolalipids derived from *Archaea* are difficult to obtain in pure form on even the 1 mg scale. We report three synthetic archaeal bolalipid mimics that retain key structural motifs of naturally occurring bolalipids yet can be readily produced in >100 mg quantities: 2,2′-di-*O*-decyl-3,3′-di-*O*-(1″,20″-eicosanyl)-bis-(*rac*-glycero)-1,1′-diphosphocholine ($C_{20}BAS^1$), 2,2′-di-*O*-hexadecyl-3,3′-di-*O*-(1″,32″-dotriacontanyl)-bis-(*rac*-glycero)-1,1′-diphosphocholine ($C_{32}BAS$), and 2,2′-di-*O*-(3,7,11,15-tetramethylhexadecyl)-3,3′-di-*O*-(1″,32″-dotriacontanyl)-bis-(*rac*-glycero)-1,1′-diphosphocholine ($C_{32}phytBAS$) (Figure 1). Each of these bolalipid structures is acyclic, symmetric, contains glycerophosphocholine headgroups, and possesses either 20 or 32 carbon transmembrane chains to stabilize the hydrophobic domains of integral membrane proteins. The hydrophobic chains at each *sn*-2 position of the bolalipid glycerol backbone are both *n*-alkyl or phytanyl, with lengths that are half that of the transmembrane chain. Methyl branching was designed into the $C_{32}phytBAS$ structure because it was expected that the phytanyl chains would lower the bolalipid gel-to-liquid-crystalline phase transition temperature relative to $C_{32}BAS$ by disrupting the alkyl chain packing within the membrane.

In this article, the first successful reconstitution of an integral membrane protein in synthetic bolalipid vesicles and the correlation of its activity with the physical properties of the membrane is demonstrated. The only prior reports of integral membrane protein enzymes in bolalipid vesicles described the use of the polar lipid extract from the thermophile *S. acidocaldarius* to functionally reconstitute beef heart cytochrome *c*-oxidase (*16*) and the leucine transporter of *Lactococcus lactis* (*17*). These studies, however, did not provide insight into the role of bolalipid structure and physical properties on the function of these membrane proteins.

The isoprenylcysteine carboxyl methyltransferase (Icmt) from *Saccharomyces cerevisiae*, Ste14p, was chosen for functional reconstitution into bolalipid membranes. Ste14p is a 26 kDa integral membrane protein with six transmem-

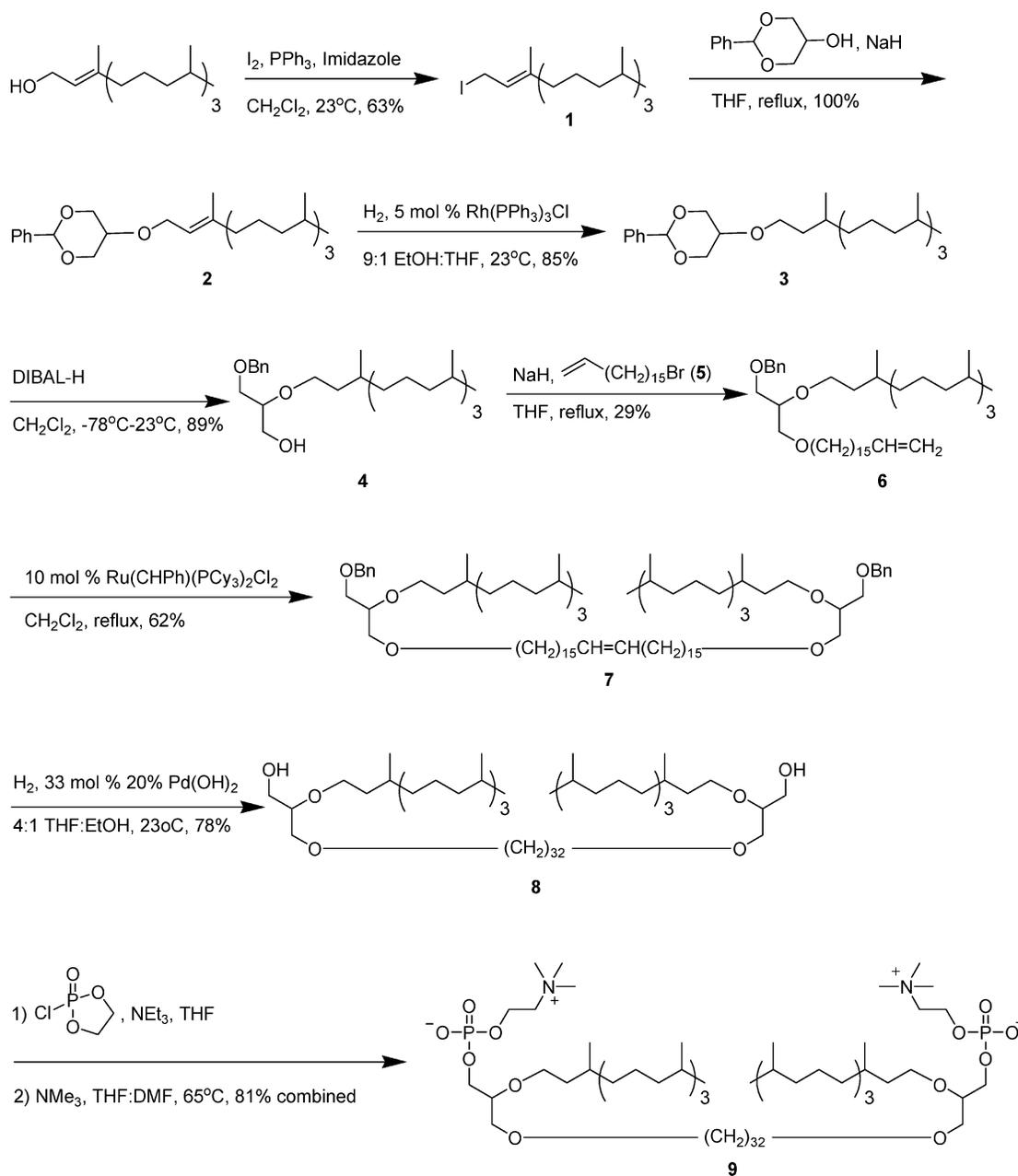Scheme 1:   Topology Model of Ste14p, Adapted from Ref 18 (*18*)
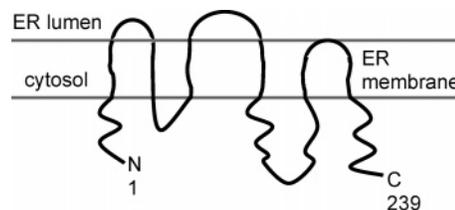
brane domains and a predicted topology as shown in Scheme 1 (*18*). Icmt is a polytopic endoplasmic reticulum membrane-localized enzyme that is responsible for the carboxyl methylation of *C*-terminal CaaX sequences (C is cysteine, "a" is generally an aliphatic residue, and X can be one of many amino acids). Carboxyl methylation of CaaX sequences is essential for the proper localization and transformation ability of oncogenic Ras proteins, thus making it an important target for chemotherapeutic agent discovery. We used the 37 kD $His_{10}myc_3$-tagged variant of Ste14p as a model enzyme for human Icmt in this study because (1) they are functional homologs (*19*) and (2) it has previously been successfully purified and functionally reconstituted in vesicles of *E. coli* polar lipids (*20*). A supported membrane sensor constructed from human Icmt-containing bolalipids may be useful for screening Icmt inhibitor candidates; therefore, reconstitution of functional Ste14p in bolalipid vesicles is an essential first step toward the development of a sensor based on this enzyme. Unfortunately, to date, attempts at purifying and functionally reconstituting human and other mammalian Icmts have met with limited to no success (*21−24*).

This contribution describes the characterization of $C_{20}BAS$, $C_{32}BAS$, and $C_{32}phytBAS$ by differential scanning calorimetry (DSC), temperature-dependent ^{31}P NMR, and fluorescence recovery after photobleaching (FRAP). The impact of bolalipid structure and membrane composition on Ste14p activity, monitored by an *in vitro* vapor diffusion methyltransferase assay (*20*), was then determined using vesicles of differing lipid composition, gel-to-liquid-crystalline phase transition temperatures, and lipid mobility. Confocal immunofluorescence microscopy and protein assays were used to determine the extent and distribution of Ste14p in reconstituted vesicle membranes. Our results show that Ste14p activity is sensitive to hydrophobic mismatch between the bolalipid membrane and the hydrophobic surface of Ste14p; however, it is not sensitive to the phase state of the host membrane. These findings suggest that $C_{32}phytBAS$ is an excellent candidate for a rugged host membrane material for Ste14p sensor production.

MATERIALS AND METHODS

Materials. The synthesis of $C_{20}BAS$ has been previously described (*25, 26*). $C_{32}phytBAS$ and $C_{32}BAS$ were synthesized as described below. POPC (1-palmitoyl-2-oleoyl-*sn*-glycero-3-phosphocholine), DMPC (1,2-dimyristoyl-*sn*-glycero-3-phosphocholine), cholesterol (Chol), *E. coli* polar lipid extract, and 1-oleoyl-2-[6-[(7-nitro-2−1,3-benzoxadiazol-4-yl)amino]hexanoyl]-*sn*-glycero-3-phosphocholine (NBD-OPPC) were purchased from Avanti Polar Lipids (Alabaster, AL). Fluorescein-labeled anti-*myc*-FITC mouse antibodies were obtained from Invitrogen (Carlsbad, CA). *N*-Acetyl-*S*-farnesyl-L-cysteine (AFC) was provided by Dr. Richard

Scheme 2: Synthesis Pathway for C_{32}phytBAS

tography was performed with 230−400 mesh silica gel using HPLC-grade eluents. Electrospray mass spectrometry (ESI MS) was performed using a Waters ZQ spectrometer. Thin layer chromatography was performed using Baker-flex IB-F plates (J.T. Baker) and visualized using UV, I$_2$ adsorption, KMnO$_4$/heat, and/or H$_2$SO$_4$/heat.

Synthesis of C$_{32}$phytBAS. The synthesis route for C$_{32}$-phytBAS (Scheme 2) was adapted from a method described for the preparation of C$_{20}$BAS (*25, 26*).

(E)-1-Iodo-3,7,11,15-tetramethylhexadec-2-ene (1). A flame-dried flask was charged with PPh$_3$ (1.0557 g, 4.04 mmol) followed by 11 mL of CH$_2$Cl$_2$ and imidazole (0.2776 g, 4.04 mmol). The solution was cooled to 0 °C, I$_2$ crystals (1.0273 g, 4.04 mmol) were added slowly, and the mixture was stirred at 25 °C for 15 min under Ar. Phytol (1.0 g, 3.37 mmol) in 3 mL of CH$_2$Cl$_2$ was then added and the mixture stirred at 25 °C under Ar for an additional 2 h. Then, petroleum ether (200 mL) was added and the mixture filtered twice through

a 1 inch pad of silica gel. After solvent removal, 0.874 g of **1** (63% yield) was obtained as a light-yellow oil. ^{1}H NMR (300 MHz, CDCl$_3$): 0.88 (t, 12 H, CH$_3$); 0.99–1.41 (m, 19 H, CH+CH$_2$ aliphatic); 1.63 (s, 3 H, CH$_3$ vinylic); 1.98 (t, 2 H, CH$_2$ allylic); 3.94 (d, 2H, CH$_2$I); 5.532 (t, 1 H, CH vinylic). ^{13}C NMR (75 MHz, CDCl$_3$): 4.10, 15.71, 19.71, 19.77, 22.63, 22.73, 24.47, 24.80, 24.91, 27.98, 32.66, 32.80, 36.43, 37.29, 37.36, 37.44, 39.38, 39.88, 121.67, 142.88. ESI$^+$ MS: *m/z* (M + H) 461.

(E)-2-Phenyl-5-O-(3,7,11,15-tetramethylhexadec-2-enyl)-1,3-dioxane (2). A flame-dried flask was charged with 2-phenyl-5-hydroxy-1,3-dioxane (0.322 g, 1.79 mmol) followed by 4 mL of THF before cooling to 0 °C. NaH dispersion (80% in oil, 0.1485 g, 4.95 mmol) was slowly added and the mixture stirred at 25 °C for 1 h. Compound **1** (0.874 g, 2.15 mmol) was dissolved in 3 mL of THF and slowly added to the alkoxide solution at 0 °C prior to heating at reflux overnight under Ar. The unreacted NaH was quenched at 0 °C with deionized H$_2$O. The aqueous phase was extracted with Et$_2$O (3 × 25 mL), and the organic phases were combined, dried over MgSO$_4$, filtered, and the solvent removed by rotary evaporation. The crude mixture was separated via column chromatography using gradient elution: 100% hexane to 1:1 hexane/CH$_2$Cl$_2$. Fractions containing the desired product were pooled, the solvent removed by rotary evaporation, and the residue dried under vacuum to give 0.879 g (100% yield) of **2** as a clear oil. ^{1}H NMR (300 MHz, CDCl$_3$): 0.86 (t, 12 H, CH$_3$); 1.05–1.57 (m, 19 H, CH+CH$_2$ aliphatic); 1.65 (s, 3 H, CH$_3$ vinylic); 1.99 (m, 2 H, CH$_2$ allylic), 3.29 (s, 1 H, CH–O); 4.01 (dd, 2 H, OCH$_2$); 4.15 (dd, 2 H, OCH$_2$ allylic), 4.31 (dd, 2 H, OCH$_2$), 5.39 (t, 1 H, CH vinylic), 5.53 (s, 1 H, OCHO acetal), 7.32 (dd, 3 H, phenyl), 7.51 (dd, 2 H, phenyl). ^{13}C NMR (75 MHz, CDCl$_3$): 16.33, 19.62, 22.53, 22.62, 24.35, 24.69, 24.97, 27.85, 32.57, 32.67, 36.58, 37.18, 37.26, 37.32, 39.26, 39.80, 64.92, 68.97, 69.16, 101.14, 120.66, 126.10, 127.97, 128.64, 138.04, 140.29. ESI$^+$ MS: *m/z* (M$^+$) 458.

2-Phenyl-5-O-(3,7,11,15-tetramethylhexadecyloxy)-1,3-dioxane (3). A flask was charged with **2** (0.12 g, 0.262 mmol) followed by 27 mL of a 9:1 EtOH/THF solution and Wilkinson's catalyst (Rh(PPh$_3$)$_3$Cl, 10 mg, 0.01 mmol). The mixture was stirred under 1 atm of H$_2$ at 25 °C overnight and filtered through a 0.5 inch pad of alumina, followed by an ~100 mL Et$_2$O rinse. The solvent was removed on a rotary evaporator and the crude product purified via column chromatography using hexane/CH$_2$Cl$_2$ as the eluent. Fractions containing the product were pooled and the solvent removed on a rotary evaporator to give 0.103 g of **3** (85% yield) as a clear oil. ^{1}H NMR (300 MHz, CDCl$_3$): 0.854 (q, 15 H, CH$_3$); 1.04–1.59 (m, 22 H, CH+CH$_2$ aliphatic); 1.68–1.72 (m, 2 H, CH$_2$ β to O); 3.25 (s, 1 H, CH–O); 3.58 (m, 2H, OCH$_2$); 4.03 + 4.33 (dd, 4 H, OCH$_2$); 5.54 (s, 1 H, CH acetal); 7.34 + 7.51 (dd, 5 H, phenyl). ^{13}C NMR (75 MHz, CDCl$_3$): 19.73, 22.60, 22.70, 24.33, 24.46, 24.77, 27.94, 29.89, 32.77, 36.70, 36.78, 37.26, 37.29, 37.42, 37.47, 39.33, 67.23, 68.97, 69.05, 70.57, 101.29, 126.16, 128.11, 128.78, 138.14. ESI$^+$ MS: *m/z* (M + H) 461.

1-O-Benzyl-2-O-(3,7,11,15-tetramethylhexadecyl)-rac-glycerol (4). A flame-dried flask was charged with **3** (2.98 g, 6.47 mmol) followed by 14 mL of CH$_2$Cl$_2$ and then cooled to −78 °C. Diisobutylaluminum hydride (DIBAL-H, 7.12 mL of a 1 M solution in CH$_2$Cl$_2$, 7.12 mmol) was added

dropwise via syringe and the reaction stirred at −78 °C for 1 h under Ar before slowly warming to 25 °C and stirring overnight. The reaction was then cooled to 0 °C and quenched with 600 μL of MeOH, and NaOH solution was added to disperse the gel (10 mL of a 5 N NaOH solution). The aqueous phase was extracted with Et$_2$O (3 × 50 mL), and the organic phases were combined, dried over MgSO$_4$, filtered, evaporated, and the residue dried under vacuum to give 2.676 g of **4** (89% yield) as a colorless oil. ^{1}H NMR (300 MHz, CDCl$_3$): 0.86 (t, 15 H, CH$_3$); 1.23 (m, 22 H, CH + CH$_2$ aliphatic); 1.56 (m, 2 H, CH$_2$ β to O); 2.34 (t, 1 H, OH), 3.63 (m, 7 H, CH–O + OCH$_2$), 4.53 (s, 2 H, OCH$_2$-Ph), 7.29 (bs, 5H, phenyl). ^{13}C NMR (75 MHz, CDCl$_3$): 19.53, 19.62, 19.68, 22.55, 22.64, 24.27, 24.40, 24.71, 27.87, 29.74, 32.70, 37.00, 37.08, 37.21, 37.24, 37.27, 37.31, 37.37, 37.42, 39.29, 62.67, 68.58, 69.92, 73.40, 78.54, 127.51, 127.56, 128.28, 137.96. ESI$^+$ MS: *m/z* (M + H) 463.

17-Bromo-1-heptadecene (5). This precursor was prepared as described by Peanasky et al. (*27*). ^{1}H NMR (300 MHz, CDCl$_3$): 1.25 (s, 24 H, −CH$_2$), 1.85 (q, 2 H, −CH$_2$), 2.25 (q, 2 H, allylic −CH$_2$), 3.40 (t, 2 H, −CH$_2$Br), 4.95 (dd, 2 H, vinyl CH$_2$), 5.8 (m, 1 H, vinyl CH). ^{13}C NMR (75 MHz, CDCl$_3$): 28.4, 29.0, 29.2, 29.4, 29.7, 29.7, 29.8, 29.8, 29.9, 29.9, 33.1, 34.0, 34.2, 76.8, 77.2, 77.7, 114.3, 139.5. ESI$^+$ MS: *m/z* (M + H) 317/319.

1-Benzyl-2-O-(3,7,11,15-tetramethylhexadecyl)-3-O-(16′-heptadecenyl)-rac-glycerol (6). A flame-dried flask was charged with **4** (2.676 g, 5.78 mmol) in 10 mL of THF and cooled to 0 °C. NaH (0.1457 g, 6.07 mmol) was added slowly and stirred at 25 °C for 1 h under Ar. A solution of **5** (5.68 g, 0.0179 mol) in 10 mL THF was slowly added at 0 °C and stirred at 25 °C for 2 days under Ar. Water (25 mL) was added and the aqueous phase extracted with Et$_2$O (3 × 50 mL). The organic phase was separated, dried over MgSO$_4$, filtered, and evaporated on a rotary evaporator. The crude product was purified by column chromatography using gradient elution: 1:1 hexane/CH$_2$Cl$_2$ to 100% CH$_2$Cl$_2$. The fractions containing the desired product were pooled, evaporated, and the residue dried under vacuum to give 1.187 g of **6** (29% yield). ^{1}H NMR (300 MHz, CDCl$_3$): 0.86 (t, 15 H, CH$_3$); 1.21 (m, 46 H, CH+CH$_2$ aliphatic); 1.57 (m, 4 H, CH$_2$ β to O); 2.03 (q, 2 H, CH$_2$ allylic), 3.54 (m, 9 H, CH–O + OCH$_2$), 4.55 (s, 2 H, OCH$_2$Ph), 4.95 (dd, 2 H, CH$_2$ vinyl), 5.81 (m, 1 H, CH vinyl), 7.29 (bs, 5 H, phenyl). ^{13}C NMR (75 MHz, CDCl$_3$): 19.74, 22.61, 22.71, 24.35, 24.47, 24.79, 26.12, 27.95, 28.94, 29.15, 29.50, 29.68, 29.78, 32.78, 33.81, 37.38, 37.45, 39.35, 68.85, 70.26, 70.72, 71.64, 73.33, 77.92, 114.06, 126.04, 127.47, 127.56, 127.67, 128.28, 139.20. ESI$^+$ MS: *m/z* (M + H) 699.

1,1′-Di-O-benzyl-2,2′-di-O-(3,7,11,15-tetramethylhexadecyl)-3,3′-di-O-(1″,32″-dotriacont-16″-enyl)-bis-(rac-glycerol) (7). A flame-dried flask was charged with **6** (1.927 g, 2.76 mmol) and 6 mL of CH$_2$Cl$_2$. Grubbs catalyst (Ru-(CHPh)(PCy$_3$)$_3$Cl$_2$, 0.2268 g, 0.276 mmol) in 5 mL of CH$_2$-Cl$_2$ was slowly added before heating the mixture at reflux overnight. After cooling the reaction mixture, the catalyst was quenched with 10 mL of H$_2$O and the aqueous phase extracted with CH$_2$Cl$_2$ (3 × 10 mL). The organic phase was then dried over MgSO$_4$, filtered, and the solvent evaporated on a rotary evaporator. The crude product was purified via column chromatography using gradient elution: 9:1 to 6:4 hexane/Et$_2$O. Fractions containing the desired product were

Scheme 3:   Synthesis Pathway for C$_{32}$BAS
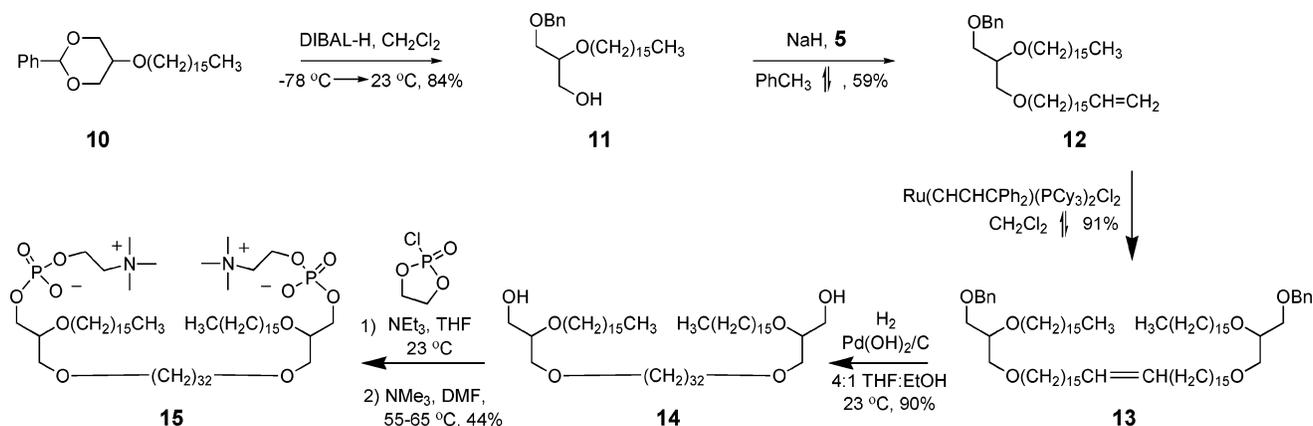
pooled, evaporated, and the residue dried under vacuum to give 1.177 g of **7** (62% yield) as a light-brown oil. ^{1}H NMR (300 MHz, CDCl$_3$): 0.86 (t, 30 H, CH$_3$), 1.25 (m, 92 H, CH+CH$_2$ aliphatic), 1.57 (m, 8 H, CH$_2$ β to O), 1.96 (c, 4 H, CH$_2$ allylic), 3.52 (m, 18 H, CH$-$O + OCH$_2$), 4.55 (s, 4 H, OCH$_2$Ph), 5.37 (m, 2 H, CH$_2$ vinyl), 7.29 (bs, 10 H, phenyl). ^{13}C NMR (75 MHz, CDCl$_3$): 19.83, 19.91, 19.96, 22.84, 22.93, 24.57, 24.70, 25.01, 26.35, 28.17, 29.40, 29.72, 29.76, 29.89, 29.92, 30.00, 32.82, 33.00, 33.31, 37.39, 37.50, 37.62, 37.67, 37.72, 39.58, 69.05, 70.52, 70.97, 71.85, 73.55, 78.17, 127.66, 127.75, 128.47, 130.06, 130.53, 138.64. ESI$^+$ MS: *m/z* (M + Na$^+$) 1393.

2,2′-Di-O-(3,7,11,15-tetramethylhexadecyl)-3,3′-di-O-(1″,- 32″-dotriacontanyl)-bis-(rac-glycerol) (8). A flask was charged with **7** (1.094 g, 0.798 mmol) followed by 25 mL of a 4:1 THF/EtOH solvent mixture and 20% Pd(OH)$_2$ on carbon catalyst (0.168 g, 0.234 mmol) and the mixture stirred under 1 atm H$_2$ at 25 °C overnight. The catalyst was removed by filtration through a 0.5 inch pad of Celite, followed by a ∼100 mL CHCl$_3$ rinse. The solvent was removed by rotary evaporation and the crude product purified by column chromatography using 3:1 hexane/Et$_2$O as the eluent. Fractions containing the desired product were pooled, evaporated, and the residue dried under vacuum to give 0.738 g (78% yield) of **8** as an ivory wax. ^{1}H NMR (300 MHz, CDCl$_3$): 0.87 (t, 30 H, CH$_3$), 1.25 (m, 100 H, CH+CH$_2$ aliphatic), 1.57 (m, 8 H, CH$_2$ β to O), 2.22 (t, 2 H, OH), 3.57 (m, 18 H, CH$-$O + OCH$_2$). ^{13}C NMR (75 MHz, CDCl$_3$): 19.97, 22.85, 22.95, 24.58, 24.71, 25.03, 26.33, 28.20, 29.72, 29.86, 29.94, 33.03, 37.37, 37.52, 37.69, 39.60, 63.32, 68.86, 71.15, 72.08, 78.51. ESI$^+$ MS: *m/z* (M + H) 1192.

2,2′-Di-O-(3,7,11,15-tetramethylhexadecyl)-3,3′-di-O-(1″,- 32″-dotriacontanyl)-bis-(rac-glycero)-1,1′-diphosphocho- line (C$_{32}$phytBAS, 9). A flame-dried flask was charged with **8** (0.150 g, 0.125 mmol), followed by the addition of 0.25 mL of THF, 2-chloro-2-oxo-1,3,2-dioxaphospholane (0.15 mL, 1.13 mmol), and Et$_3$N (0.12 mL, 0.565 mmol). The turbid mixture was diluted with 2 mL of THF and 1 mL of DMF. The reaction mixture was then transferred to a flame-dried pressure tube and 1 mL of Me$_3$N condensed into the tube. The tube was then sealed and heated to 70 °C with stirring for 2 days. The reaction vessel was then slowly cooled to 0 °C, the pressure carefully released, and the product mixture concentrated on a rotary evaporator. The product was isolated by silica gel column chromatography using step gradient elution: 80:20:0, 0:100:0, 65:35:5, 60:

40:10 CHCl$_3$/MeOH/H$_2$O. Suspended silica particles were removed from the fractions using a 0.22 μm PTFE filter, the solvent evaporated, and the residue dried under vacuum to give 0.1903 g of **9** (81% yield) as a wax. ^{1}H NMR (300 MHz, CDCl$_3$/CD$_3$OD): 0.86 (t, 30 H, CH$_3$), 1.19 (m, 100 H, CH+CH$_2$ aliphatic), 1.53 (m, 8 H, CH$_2$ β to O); 3.23 (s, 18 H, NMe$_3$), 3.49 (m, 18 H, CH$-$O + OCH$_2$), 3.90 (t, 4 H, CH$_2$N), 4.25 (bs, 4 H, CH$_2$OP). ^{13}C NMR (75 MHz, CDCl$_3$/CD$_3$OD): 21.16, 21.24, 24.12, 24.20, 26.04, 26.37, 27.67, 29.52, 31.28, 34.37, 38.84, 39.01, 40.94, 55.76, 60.52, 66.69, 68.08, 70.43, 70.62, 72.17, 73.33. ^{31}P NMR (124 MHz, CDCl$_3$/CD$_3$OD): single peak (unreferenced) confirms the presence of a single phosphorus bonding motif. ESI$^+$ MS: *m/z* (M + H) 1522.

Synthesis of C$_{32}$BAS. The synthesis route for C$_{32}$BAS is shown in Scheme 3.

1-O-Benzyl-2-hexadecyloxy-3-O-(16′-heptadecenoxy)-rac- glycerol (12). A flame-dried flask was charged with 95% NaH dispersion in oil (0.159 g, 6.6 mmol) followed by 30 mL of toluene and cooled to 0 °C. A solution of **11** (1.51 g, 3.7 mmol) (*25, 26*) in toluene (30 mL) was added via syringe and the mixture stirred for 1 h. A solution of **5** (2.1 g, 6.6 mmol) dissolved in 20 mL of toluene was added at 25 °C via syringe and the mixture heated at reflux overnight. Water (50 mL) was added and the aqueous phase extracted with diethyl ether (3 × 50 mL), dried over MgSO$_4$, filtered, and evaporated on a rotary evaporator. The crude product was purified by column chromatography using 10:1 hexane/Et$_2$O as the eluent. The fractions collected at R_f = 0.2 were pooled, evaporated, and the residue dried under vacuum to give 2.5 g of **12** (59% yield) as a clear oil. ^{1}H NMR (300 MHz, CDCl$_3$): 0.89 (t, 3 H, $-$CH$_3$), 1.26 (s, 50 H, $-$CH$_2$), 1.57 (m, 4 H, $-$CH$_2$ β to O), 2.03 (c, 2 H, vinyl CH$_2$), 3.45 (m, 9 H, -OCH$_2$), 4.56 (s, 2 H, -OCH$_2$-Ph), 4.95 (dd, 2 H, vinyl CH$_2$), 7.33 (m, 5 H, $-$C$_6$H$_5$). ^{13}C NMR (75 MHz, CDCl$_3$): 14.3, 22.9, 22.9, 26.3, 26.4, 26.4, 29.2, 29.4, 29.6, 29.7, 29.9, 30.3, 31.8, 32.2, 34.1, 70.5, 70.8, 71.0, 71.2, 71.9, 73.6, 78.2, 114.3, 127.7, 127.8, 128.5, 138.7, 139.5. Mass (M + H) 643 by EI/CI.

1,1′-Di-O-benzyl-2,2′-di-O-hexadecyl-3,3′-di-O-(16″-dot- riacontenyl)-bis-(rac-glycerol) (13). This compound was prepared as described for **7** from **12**. The crude product was purified via column chromatography using 7:2 hexane/diethyl ether. Fractions at R_f = 0.3 were combined, evaporated, and the residue dried under vacuum to give 0.4007 g of **13** (91% yield). ^{1}H NMR (300 MHz, CDCl$_3$): 0.89 (t, 6 H, $-$CH$_3$),

1.26 (s, 25 H, $-CH_2$), 1.57 (m, 8 H, $-CH_2$ β to O), 1.97 (m, 4 H, vinyl CH_2), 3.43 (m, 18 H, $-OCH_2$), 4.56 (s, 4 H, $-OCH_2$-Ph), 5.39 (m, 2 H, vinyl CH_2), 7.33 (m, 10 H, $-C_6H_5$). ^{13}C NMR (75 MHz, $CDCl_3$): 14.1, 22.7, 23.6, 26.1, 29.2, 29.4, 29.5, 29.7, 30.1, 31.9, 32.6, 70.3, 70.6, 70.7, 71.7, 73.3, 77.9, 127.5, 127.6, 128.3, 130.3. Mass (M + Na) 1279 by MALDI.

2,2′-Di-O-hexadecyl-3,3′-di-O-(dotriacontyl)-bis-(rac-glycerol) (14). This compound was prepared as described for **8** starting from **13**. The crude product was purified via column chromatography eluting with a gradient solvent system from 4:1 to 0:100 hexane/Et_2O, followed by a column flush with 5:1 $CHCl_3$/MeOH to give **14** as a white solid (0.557 g, 90% yield). ^{1}H NMR (300 MHz, $CDCl_3$): 0.89 (t, 6 H, $-CH_3$), 1.25 (s, 108 H, $-CH_2$), 1.56 (m, 8 H, $-CH_2$ β to O), 1.89 (bs, 2 H, -OH), 3.37−3.74 (m, 18 H, $-OCH_2$, -OCH). ^{13}C NMR (75 MHz, $CDCl_3$): 14.1, 22.7, 26.1, 26.2, 29.2, 29.3, 29.5, 29.6, 29.7, 30.1, 31.9, 63.0, 70.4, 70.9, 71.8, 78.3. Mass (M + Na) 1102 by MALDI.

2,2′-Di-O-hexadecyl-3,3′-di-O-(dotriacontyl)-bis-(rac-glycerol)-1,1′-diphosphocholine (C_{32}BAS, 15). This compound was prepared as described for **9** using **14** as the precursor. The crude yellow solid obtained was purified via silica gel column chromatography using a step gradient elution with 80:20:0, 50:50:0, 0:100:0, 65:35:5, and 60:40:10 $CHCl_3$/MeOH/H_2O. The fractions containing the product were combined and extracted using the Bligh−Dyer method. The organic phase was dried with $MgSO_4$, concentrated, and further dried under vacuum to give 0.0581 g of **15** (44% yield); the remaining material was the starting diol, **14**. ^{1}H NMR (300 MHz, $CDCl_3$/CD_3OD): 0.89 (t, 6 H, $-CH_3$), 1.28 (s, 108 H, $-CH_2$), 1.57 (t, 8 H, $-CH_2$ β to O), 3.23 (s, 18 H, $N(CH_3)_3$), 3.45−3.52 (m, 6 H, $-OCH_2$, $-OCH$), 3.58−3.64 (m, 12 H, $-OCH_2$, $-OCH$), 3.91 (t, 4 H, $-CH_2$-NMe_3), 4.29 (bs, 4 H, $-CH_2$-OP). ^{13}C NMR (75 MHz, $CDCl_3$/CD_3-OD): 24.4, 27.8, 31.1, 31.3, 31.4, 31.8, 33.6, 55.9, 72.4. ^{31}P NMR (124 MHz, $CDCl_3$/CD_3OD): one unreferenced peak. Mass (M + H) 1411 by MALDI.

DSC. Calorimetric experiments were performed on a TA DSC-Q10 instrument using 1 mg lipid/4 mg H_2O in stainless steel pans. All thermograms were run using a reference pan with H_2O. Indium was used as a calibration standard. Thermograms were collected in the heating mode using a scan rate of 1 °C/min. The temperatures scanned ranged from −20 to 85 °C. Three thermograms were collected and the average values for the transition temperature (determined at the transition peak) reported.

^{31}P NMR Chemical Shift Anisotropy. Proton-decoupled ^{31}P NMR spectra were acquired at temperatures from −5 to 30 °C to determine the change in chemical shift anisotropy of the ^{31}P powder pattern line shape for C_{32}phytBAS. The sample was prepared by hydrating a dry film of C_{32}phytBAS at a concentration of 20 mg/mL in D_2O. Spectra were obtained using a Bruker DRX 500 spectrometer equipped with a 5 mm probe. A period of 15 min was allowed for temperature equilibration before spectral acquisition at each temperature studied. All spectra were acquired using the following parameters: 1600 scans, relaxation delay of 1 s, 90° pulse duration of 6 μs, acquisition time of 0.2 s, and 200 Hz line broadening. The peak width at half the peak height was measured for each spectrum and the results plotted in ppm versus temperature. The intersection of the two linear

regions in this plot was taken as the T_m.

FRAP. Standard coverslips were cleaned with warm 7:1 Triton X100/H_2O for 10 min, rinsed extensively with deionized H_2O, dried under a stream of N_2, and baked at 400 °C for 5 h. Vesicles of POPC, POPC/C_{20}BAS (100 nm nominal diameter), C_{20}BAS, and C_{32}phytBAS (200 nm nominal diameter) were prepared by extrusion as described below, except that 18 MΩ H_2O was used instead of the buffer, and the extrusions were done at 65 °C. Total lipid concentrations were 5 μmol/mL at lipid ratios of 99.5% lipid + 0.5% NBD-OPPC. The vesicle solutions were mixed with 300 mM NaCl (1:1 v/v) and transferred to a perfusion chamber mounted on the coverslips. After approximately 1 min, the coverslips were dipped into a 18 MΩ H_2O bath and a cover glass sandwich prepared. The sandwich was quickly placed on a microscope holder with H_2O pools on both sides. A detailed description of this method for preparing supported lipid bilayers from vesicles has been reported elsewhere (*28, 29*).

A Nikon TE200U fluorescence microscope coupled to a silicon avalanche photodiode and a continuous wave argon ion laser (488 nm emission, 25 mW) was used to both bleach and excite the NBD-OPPC probe (λ_{ex} = 460 nm, λ_{em} = 534 nm). A neutral density filter was placed in the beam path to reduce the laser intensity to 250 nW to avoid constant photobleaching of the probe. A shutter in the beam path was pulsed to enable detection of the initial fluorescence counts for ~40 s. Upon removal of the filter from the beam path, the shutter sends a single photobleaching laser pulse for ≤1 s (bleach radius = 13 μm). The recovery of fluorescence intensity in this photobleached area is then monitored as a function of time. Diffusion coefficients of NBD-OPPC in various membrane compositions were determined by measuring the half-time to recovery using a modified Bessel function as described by Soumpasis (*30*). All of the data were fit as a single exponential and compared to POPC as the standard. Diffusion coefficients determined in this manner are accurate to ±15%. All FRAP measurements were conducted at 25 °C.

Vesicle Preparation. Dry lipid (10 mg) was dissolved in 1:1 $CHCl_3$/MeOH in a cryovial and a thin film produced from it by evaporating the solvent under a gentle stream of Ar. The solvent was further removed under a 100 μm vacuum overnight. After the addition of 1 mL of 100 mM TRIS HCl at pH 7.5, the solution was subjected to five cycles of freeze (liquid N_2 bath), thaw (water bath at 35 °C for 5 min), and vortex (30 s) to give a polydisperse MLV suspension as described by DiMeglio et al. (*31*). This dispersion was extruded twenty times at 25 °C through two stacked 100 nm pore track-etch filters to produce an almost transparent solution. All samples were prepared similarly and were analyzed immediately after preparation.

Purification of Ste14p from Membranes. Ste14p with 10 histidine residues and 3 repeats of the *myc* epitope at the *N*-terminus was expressed and purified as previously described (*20*). The histidines were used to facilitate Ste14p purification, and the *myc* epitopes were used for immunodetection. Briefly, $His_{10}myc_3$-tagged Ste14p was expressed in *S. cerevisiae*, extracted from crude membranes using 1% (w/v) 1-β-D-dodecylmaltopyranoside (DDM), and purified using Talon metal affinity chromatography. The activity of the pure enzyme was measured using AFC as the model

substrate in an *in vitro* vapor diffusion methyltransferase assay (see below). Protein concentrations were determined by an amido black protein assay (*32*).

Reconstitution of Ste14p in Mixed Lipid Vesicles. Purified Ste14p was reconstituted by rapid dilution in the presence of lipid dispersions as previously described (*20*). Briefly, ~1 μg of protein was added to 10 μL of a 10 mg/mL vesicle solution, and a subsequent 20-fold rapid dilution was performed by the addition of 100 mM Tris-HCl buffer at pH 7.5 at 5 °C.

Vapor Diffusion Methyltransferase Assay in Vitro. The assay was performed as described by Anderson et al. (*20*). The buffer, vesicle solution, protein, and assay reagents were temperature-equilibrated on ice prior to the addition of 1 μg of Ste14p to 10 μL of vesicle solution followed by the addition of 200 μM AFC. The samples were incubated on ice for 5 min followed by rapid dilution with buffer and the addition of 20 μM [^{14}C]-SAM to a final volume of 60 μL. The reaction solution was incubated in a water bath at 30 °C and the reaction allowed to progress for 30 min. The methyl transfer reaction was quenched by the addition of 50 μL of 1 M NaOH/1% SDS. The mixture (100 μL) was then spotted on filter paper and placed in the neck of a scintillation vial that contained 10 mL of BioSafe II scintillation cocktail. After 2.5 h, the filters were removed and the NaOH-labile counts determined by liquid scintillation. The results are reported in pmol of methyl groups transferred/mg protein/min of reaction.

Temperature-Dependent Methyltransferase Assays. Vapor diffusion methyltransferase assays were performed *in vitro* at different temperatures to test the effect of the lipid phase transition temperature on protein activity. Ste14p was reconstituted at 32 °C into *E. coli* polar lipid, DMPC, or C$_{20}$BAS liposomes. Vapor diffusion methyltransferase experiments were done *in vitro* as previously described with the exception that the incubation temperature was changed to 10 °C, 16 °C, 32 °C, or 44 °C as needed to probe Ste14p activity above and below the phase transition temperature of the host membrane.

Confocal Immunofluorescence Microscopy. Ste14p (10 μL of a 0.012 μg/μL solution in 500 mM imidazole elution buffer) was diluted to a final volume of 200 μL in 100 mM Tris-HCl buffer at pH 7.5 containing unextruded vesicles (1 μL of a 10 μg/μL solution). The protein was stained by the addition of an anti-*myc* monoclonal mouse antibody followed by the addition of a fluorescein isothiocyanate-conjugated goat anti-mouse secondary antibody (0.1 μL of 1 μg/μL solution). Nile Blue was then added to stain the membrane, and the samples were imaged at 60× magnification.

RESULTS

Synthesis. C$_{32}$phytBAS was prepared as shown in Scheme 2 on the basis of the previously described syntheses of C$_{20}$-BAS and C$_{32}$BAS (*24–26*). Phytanyl iodide, prepared by the iodination of phytol in the presence of triphenylphosphine and imidazole, was coupled with 2-phenyl-5-hydroxy-1,3-dioxane to produce ether **2** in quantitative yield. The phytanyl olefin was hydrogenated in the presence of Wilkinson's

Table 1: Gel-to-Liquid-Crystalline Phase Transition Temperatures for Hydrated Bolalipids Determined by Differential Scanning Calorimetry

bolalipid	T_m (°C)
C$_{32}$phytBAS	14 ± 0.1
C$_{20}$BAS	17 ± 0.3
C$_{32}$BAS	>85

catalyst in 85% yield. Reductive ring opening of the dioxane ring with DIBAL-H (*33*) gave the 2-phytanyl-1-benzyl-*rac*-glycerol diether (**4**) in 89% yield. Alkylation of the primary alcohol in **4** with **5** (*27*) gave the corresponding benzyl-protected glyceryl triether **6** in 29% yield. Dimerization of **6** via olefin metathesis using the first-generation Grubbs catalyst (*34*) gave **7** in 62% yield. Simultaneous olefin reduction and deprotection of **7** was achieved using Pd(OH)$_2$-catalyzed hydrogenolysis. The phosphocholine headgroup was installed in the final step using a 2-chloro-2-oxo-1,3,2-dioxaphospholane esterification/trimethylamine ring opening sequence (*35*, *36*) to give the methyl-substituted bolalipid C$_{32}$phytBAS (**9**) in 81% yield (2% overall yield).

The synthesis route for C$_{32}$BAS (Scheme 3) followed a similar path. 2-Phenyl-5-hexadecyloxy-1,3-dioxane (**10**), prepared as described by Patwardhan and Thompson (*25*, *26*) in 79% yield, was subjected to reductive ring opening with DIBAL-H (*33*) to give **11** in 84% yield. 17-Bromo-1-heptadecene (**5**) was used to alkylate **11** in 59% yield. Intermediate **13** was obtained in 91% yield via dimerization of **12** using Grubbs catalyst (*34*). The simultaneous deprotection and reduction of this precursor gave the tetraether bisglycerol intermediate **14** in 90% yield. Installation of the phosphocholine headgroups as before produced C$_{32}$BAS (**15**) in 44% yield (14% overall yield).

Phase Transition Behavior of C$_{32}$phytBAS and C$_{32}$BAS Dispersions. The DSC data obtained for hydrated C$_{32}$-phytBAS, C$_{20}$BAS, and C$_{32}$BAS in sealed pans is summarized in Table 1. C$_{20}$BAS was previously reported to have a T_m value of 17 °C as determined by DSC and temperature-dependent Raman spectroscopy (*31*). DSC experiments revealed that the gel-to-liquid-crystalline phase transition of C$_{32}$phytBAS was 14 °C (Figure 2A) and was undetectable up to 85 °C for C$_{32}$BAS (data not shown). Changes in the chemical shift anisotropy of C$_{32}$phytBAS, determined by temperature-dependent ^{31}P NMR (Figure 2B), also indicated that the T_m for this bolalipid was 14 °C.

Lateral Diffusion Rates of C$_{32}$phytBAS Dispersions. Work by Thompson and co-workers (*37*) has shown that the lateral diffusion coefficients for POPC, C$_{20}$BAS/POPC, C$_{20}$BAS, and 7:3 C$_{20}$BAS/Chol on detergent cleaned and baked cover glass are 8 × 10^{-8} cm^2/s, 4 × 10^{-8} cm^2/s, 1.5 × 10^{-8} cm^2/s, and 1.2 × 10^{-9} cm^2/s, respectively. Our FRAP data for glass-supported bolalipid membranes showed that the lateral diffusion rate of pure C$_{32}$phytBAS (1.8 × 10^{-9} cm^2/s, Table 2) was an order of magnitude slower than that observed for the unbranched shorter chain variant, C$_{20}$BAS (1.5 × 10^{-8} cm^2/s, Table 2) and similar to that observed for 7:3 C$_{20}$BAS/Chol (1.2 × 10^{-9} cm^2/s, Table 2).

Vapor Diffusion Methyltransferase Assays in Vitro. Vapor diffusion methyltransferase assays (Scheme 4) *in vitro* demonstrated that when the molar ratio of C$_{20}$BAS was increased in *E. coli* polar lipid membranes, Ste14p activity was retained until the C$_{20}$BAS content in the membrane
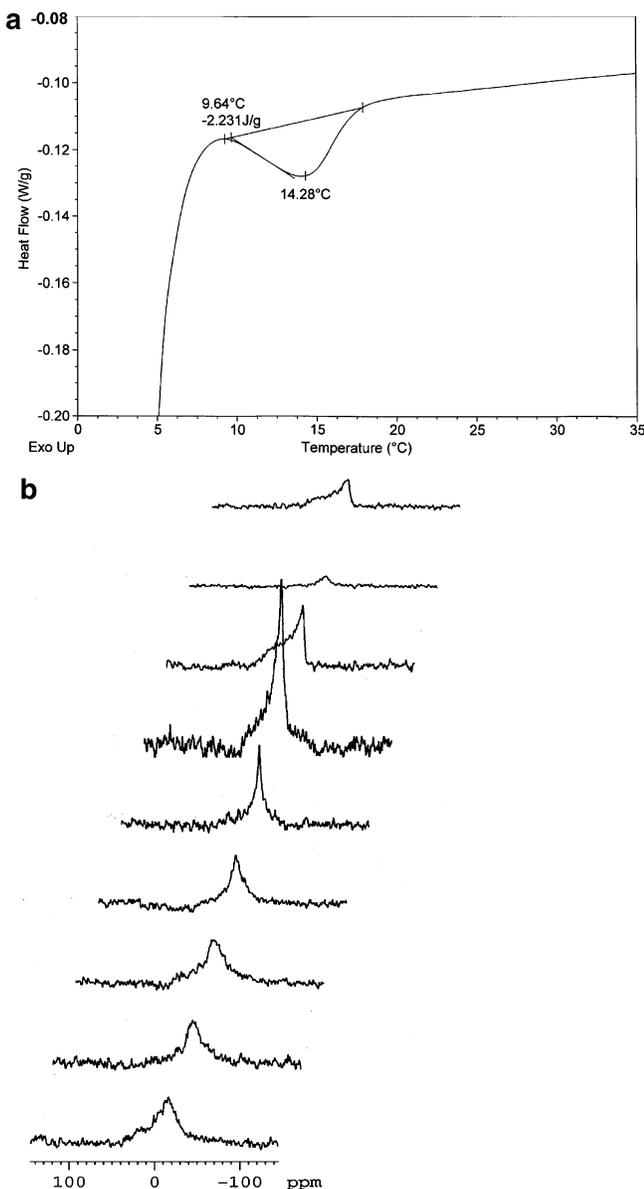
a

b

FIGURE 2: Phase transition behavior of C_{32}phytBAS. (A) DSC of C_{32}phytBAS dispersion (1 mg lipid/4 μL H_2O) in sealed stainless steel pans with a heating rate of 1 °C/min. One out of three trials is shown. The phase transition temperature (T_m = 14.3 °C) and transition enthalpy (−2.23 J/g) are displayed. (B) Temperature-dependent proton-decoupled ^{31}P NMR spectra of C_{32}phytBAS in D_2O. Top to bottom: 30, 25, 20, 15, 12, 10, 5, 0, −5 °C. The lipid was hydrated (20 mg of lipid/1 mL of D_2O) and extruded through 200 nm track-etch membranes. Typically, 1600 scans were acquired with a relaxation delay of 1 s, 90° pulse of 6 μs, and an acquisition time of 0.2 s. The spectra were processed with a line broadening of 200 Hz.

exceeded 50 mol % (Figure 3A). At 3:1 C_{20}BAS/*E. coli* polar lipid, only 15% methyltransferase activity remained, and only 3% activity remained in pure C_{20}BAS. A similar variation of membrane composition using C_{32}phytBAS showed that Ste14p activity was retained in all molar ratios tested such that pure C_{32}phytBAS vesicles possessed 80% of the Ste14p methyltransferase activity found in Ste14p vesicles reconstituted with pure *E. coli* polar lipid extract.

When POPC was used as the host membrane lipid instead of *E. coli* polar lipid, the Ste14p activity dropped to 47% of its level in 100% *E. coli* polar lipid (Figure 3B). Ste14pactivity gradually dropped as the C_{20}BAS composition in POPC

Table 2: Lateral Diffusion Coefficients of NBD-OPPC in Lipid Membranes on Glass, Determined by FRAP

lipid	D (cm^2/s)
POPC	8.0 (± 2.2) × 10^{-8}
C_{20}BAS:POPC	3.6 (± 0.3) × 10^{-8}
C_{20}BAS	1.5 (± 0.1) × 10^{-8}
7:3 C_{20}BAS:chol	0.12 (± 0.03) × 10^{-8}
C_{32}phytBAS	0.18 (± 0.03) × 10^{-8}

increased to 1:1 C_{20}BAS/POPC. Further increases in the C_{20}-BAS molar ratio, however, caused a drop in the methyltransferase activity to 16% and 4% of the pure POPC level for 3:1 and 100:0 C_{20}BAS/POPC compositions, respectively. When the same bolalipid composition variation experiment was performed with C_{32}phytBAS in POPC, Ste14p activity was retained at levels similar to or greater than that of pure POPC dispersions regardless of C_{32}phytBAS content in the membrane. It should be noted that the slight difference in Ste14p specific activity observed in both 100% C_{32}phytBAS dispersions (Figure 3A and B) is due to the different Ste14p preparations used in these two series of experiments. Nonetheless, all bolalipid/*E. coli* polar lipid data were collected with a single Ste14p preparation, whereas all bolalipid/POPC data were collected with another Ste14 preparation to eliminate this difference as a variable within a set of lipid mixtures.

To further probe the influences of lipid physical properties on Ste14p function, we monitored its methyltransferase activity in lipids above and below their gel-to-liquid-crystalline phase transition after reconstitution at a single temperature (32 °C) (Table 3). For the *E. coli* polar lipid (control), Ste14p activity remained essentially constant when the assay temperature was maintained at 10, 16, 32, or 44 °C. The methyltransferase activity in DMPC was unchanged below (16 °C) and above (32 °C) its phase transition temperature (T_m = 23 °C), yielding activity levels that were the same as the *E. coli* polar lipid values within experimental error. Dramatically different behavior was found for C_{20}-BAS, however. In this case, the methyltransferase activity was only 5% of that observed for the *E. coli* polar lipid above (32 °C) and below (10 °C) the phase transition temperature of C_{20}BAS (T_m = 17 °C).

Confocal immunofluorescence assays were performed to determine whether Ste14p was actually incorporated within the membrane dispersions where low methyltransferase activity was observed (Figure 4). Fluorescence and phase contrast images were collected on reconstituted vesicle samples prepared as described above, except that mouse anti-*myc* primary antibodies and FITC-labeled goat anti-mouse secondary antibodies were added to fluorescently labeled Ste14p, and Nile Blue was added as a membrane-localizing fluorophore. As the data in Figure 4 demonstrate, Ste14p was present in all reconstituted vesicle compositions, including those showing low methyltransferase activity (i.e., C_{20}-BAS).

DISCUSSION

The goal of this study was to determine the optimal host membrane material in which to functionally reconstitute the Icmt enzyme, Ste14p, for use in a stable supported membrane sensor. The design rules for producing stable integral
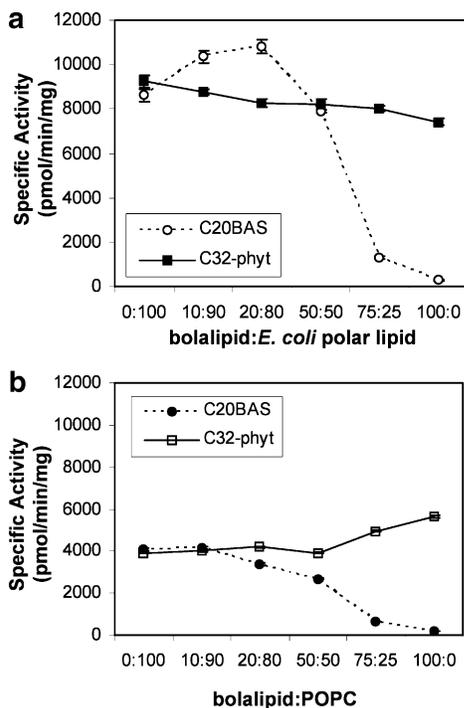
FIGURE 3: Ste14p methyltransferase activity vs bolalipid/*E. coli* polar lipid composition (A) and bolalipid/POPC composition (B). Ste14p (~1 μg) was added to 10 μL of vesicle dispersion followed by 200 μM AFC and rapid dilution by the addition of 20 μM [^{14}C]-SAM. The samples were then incubated for 30 min at 30 °C before quenching with 50 μL of 1 M NaOH/1% SDS. The mixture was spotted on a filter paper and analyzed by the vapor diffusion assay for 2.5 h as described in the Materials and Methods section. Specific activities were plotted as pmol of methyl groups transferred/mg of protein/min.

Table 3: Specific Activity of Ste14p (pmol/min/mg) as a Function of Lipid Type and Their Gel-to-Liquid-Crystalline Phase Transition Temperatures[a]

lipid	T_m (°C)	specific activity, below T_m (assay temp., °C)	specific activity, above T_m (assay temp., °C)
E. coli polar lipid	6–24[b]	6240 (10)	
E. coli polar lipid	6–24		6820 (30)
E. coli polar lipid	6–24		7140 (32)
E. coli polar lipid	6–24		6560 (44)
C_{20}BAS	17	290 (10)	310 (32)
DMPC	23	6450 (16)	6630 (32)

[a] Ste14p reconstitutions in all lipid types were all conducted at 32 °C; the methyltransferase reactions were subsequently incubated at the temperatures indicated in parentheses for each lipid measured. The precision of the specific activity measurements are ±3%. [b] M. Esfahani et al. (1971) *Proc. Natl. Acad. Sci. U.S.A. 68*, 3180.

membrane-protein-containing membranes are not yet clear. For example, some integral membrane protein enzymes such as Ca^{2+}-ATPase do not retain their functional conformation in gel phase lipid bilayers (*38*). However, not all membrane proteins display higher activities in the liquid-crystalline phase membranes, particularly when the liquid crystalline membrane phase is too thin to accommodate the entire hydrophobic surface of the protein. This is the case with diacylglycerol kinase and Na$^+$, K$^+$-ATPase (*39, 40*), both of which undergo activity enhancements when the host membrane thickens upon transition from the liquid crystalline to gel phase. In some other cases, the proteins themselves affect the transition temperature of the surrounding lipids to relieve hydrophobic mismatch between the membrane and the integral membrane protein (*41*). The function of bacteriorhodopsin (bR)-containing membranes, however, is highly dependent on membrane fluidity. bR in polymerized synthetic bilayer membranes is inactive (*42, 43*), whereas bR in bilayers composed of naturally occurring lipids shows a strong dependence on the site and degree of acyl chain unsaturation (*44*). Taken together, these studies show that integral membrane protein activity can be strongly influenced

in unpredictable ways by the phase behavior, physical dimensions, and fluidity of the host membrane.

An existing bolalipid, C_{20}BAS, and two newly synthesized bolalipids, C_{32}BAS and C_{32}phytBAS (prepared in 14% and 2% overall yield, respectively), were used to probe the structure–activity relationship between bolalipid structure and Ste14p function. DSC and ^{31}P NMR data show that C_{32}phytBAS and C_{20}BAS form liquid crystalline membranes at 25 °C; however, C_{32}BAS is in the gel phase at this temperature and did not have an observable melting transition over the temperature range studied (15–85 °C). Methyl branching of the *sn*-2 chains in C_{32}phytBAS disrupts the alkyl chain packing of this bolalipid, thereby increasing membrane fluidity and lowering the gel-to-liquid-crystalline phase transition temperature and the transition enthalpy relative to C_{32}BAS. The observed phase transition temperature of C_{32}-phytBAS, T_m = 14 °C, is in reasonable agreement with the value of 8 °C reported by Kinoshita and co-workers, who also prepared this bolalipid (*45, 46*). Differences in sample preparation methods, the presence of contaminants, or different thermal history of the samples may account for the lower temperature reported in the previous work. The T_m of C_{20}BAS has been previously reported to be 17 °C (*31, 37*). The absence of methyl branching in C_{20}BAS and the shorter membrane-spanning alkyl chain length (C_{20} vs C_{32}) are factors that compensate each other to produce a bolalipid with a modest phase transition temperature in this case. The T_m values measured for this bolalipid series are summarized in Table 1.

Lateral diffusion rates of the liquid-crystalline bolalipids, determined using the FRAP technique for supported membrane samples, are summarized in Table 2 along with the control lipid, POPC. The diffusion rate obtained for C_{20}BAS was slower by a factor of 5 relative to POPC under the same conditions. When 30 mol % Chol was incorporated into the C_{20}BAS membrane, the observed lateral diffusion rate decreased by an order of magnitude, giving a value similar to that obtained for the longer chain C_{32}phytBAS

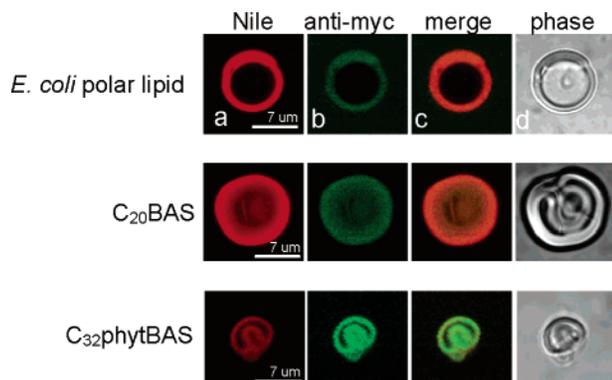Scheme 4: Vapor Diffusion Assay Reaction
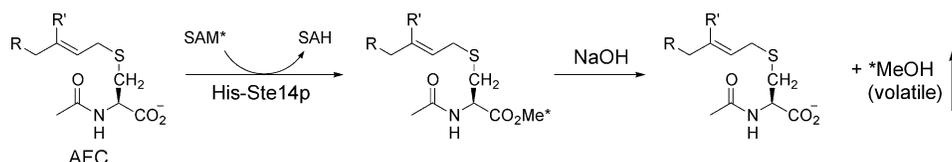
FIGURE 4: Confocal immunofluorescence microscopy of giant vesicles of *E. coli* polar lipid (top), $C_{20}BAS$ (middle row), and C_{32}-phytBAS (bottom row). Nile Blue was added to stain the membranes (column a) and Ste14p was stained with mouse anti-*myc*/goat FITC-anti-mouse antibodies (column b). The images from a and b were merged (column c); the phase contrast images appear in column d. Ste14p was reconstituted into unextruded vesicles for these experiments and imaged at 60× magnification.
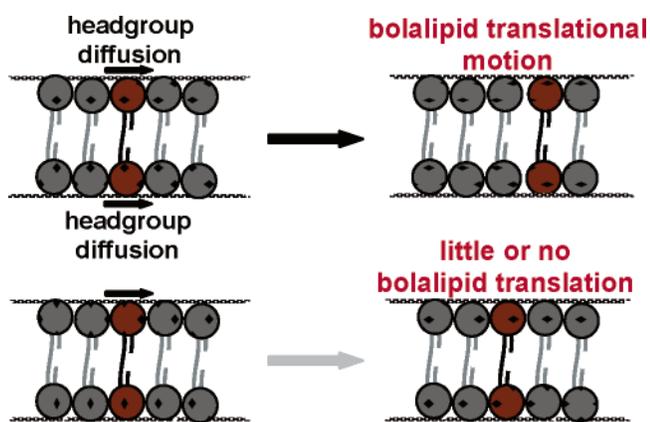

FIGURE 5: Conceptual diagram of the headgroup-coupled diffusion of bolalipids, indicating the different outcomes of cooperative and uncooperative headgroup motions at the opposing membrane−water interfaces.

derivative. FRAP measurements were not possible with C_{32}-BAS because its I_m was greater than 85 °C. This bolalipid produced glass-supported membranes where only punctate fluorescence was observed, indicative of fluorophore-rich domains that were phase separated from the gel phase bolalipid. We infer from these results that the reduced rates of diffusion in bolalipid membranes, relative to those of monopolar lipids that form bilayer membranes, is caused by the coupled diffusion of headgroups at opposing lipid-water interfaces in the monolayer membranes formed by bolalipids (Figure 5). An alternative explanation is based on the consideration of lipid size. Because methyl branching increases the lipid molecular area at the lipid−water interface relative to its unbranched counterpart (*45*), the diffusion path length of these larger diameter molecules is effectivelyin-
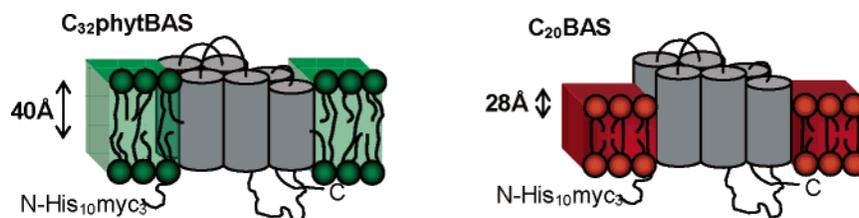
creased, thereby decreasing the net diffusion rate. Our observed diffusion rate of 1.8×10^{-9} cm^2/s for C_{32}phytBAS is in reasonable agreement with the reported value of 7×10^{-9} cm^2/s for a biogenic bolalipid extract (9:1 bolalipid/monopolar lipid), determined at 30 °C by 2D exchange ^{31}P NMR (*47*). A key finding from these experiments is that the slower bolalipid lateral diffusion rates did not significantly impact methyltransferase activity in the functional reconstitution of Ste14p within bolalipid vesicles. Although there is no literature on this subject as far as we know, we anticipated that a change in lipid lateral diffusion rate would lead to changes in membrane microviscosity that would ultimately impact Ste14p activity. Our data suggest that Ste14p is not sensitive to these types of membrane perturbations.

Confocal immunofluorescence microscopy further shows that the properties of the lipid do not alter the capacity for Ste14p incorporation within the host membrane (i.e., Ste14p is incorporated within both gel and liquid crystalline phase membranes as well as hydrophobically mismatched membranes). Consistent with this finding, protein assay results confirmed the presence of Ste14p in the membrane, regardless of lipid type. Because the hydrated membrane thicknesses for $C_{20}BAS$, $C_{32}BAS$, and C_{32}phytBAS are 32 Å (*31*), 56 Å, and 50 Å, respectively, we conclude that the lower levels of methytransferase activity observed in $C_{20}BAS$ vesicles is caused by mismatch of the hydrophobic domain of Ste14p (anticipated to be on the order of 40 Å thick) and the ~28 Å thick hydrophobic region of the $C_{20}BAS$ membrane (Figure 6). This hydrophobic mismatch may lead to misfolded and/or denatured Ste14p segments in the thinner $C_{20}BAS$ membranes, thereby accounting for the lower methyltransferase activity observed.

CONCLUSIONS

Hrycyna and co-workers (*20*) have previously shown that Ste14p can be reconstituted in vesicles with a variety of different monopolar lipid types while retaining greater than 60% of the activity present in *E. coli* polar lipid extract vesicles. We now report that a large amount of Ste14p activity was retained (65% or higher) in membranes composed of ≤50 mol % $C_{20}BAS$; however, methyltransferase activity decreases rapidly at higher molar ratios of $C_{20}BAS$. Ste14p activity levels were maintained across the full 0−100 mol % range of C_{32}phytBAS/*E. coli* polar lipid extract compositions. Surprisingly, gel phase lipids do not appear to negatively affect methyltransferase activity on the basis of our findings that gel phase lipids (DMPC vesicles at 16 °C) and liquid crystalline phase lipids (C_{32}phytBAS and DMPC vesicles at 25 °C and 32 °C, respectively) yield similar activities at membrane compositions of ≤50 mol % bolalipid. The thickness of the hydrophobic region of the membrane, however, does appear to have a significant impact

FIGURE 6: Illustration of the hydrophobic mismatch and match between $C_{20}BAS$ and C_{32}phytBAS bolalipids and Ste14p, respectively.

on Ste14p activity, with the thinner C_{20}BAS membrane producing a less active reconstituted Ste14p vesicle dispersion. Additional experiments to probe this question and an extension of these studies to other classes of integral membrane proteins are in progress to determine the generality of these findings.

ACKNOWLEDGMENT

Note Added after ASAP Publication. There was an error in the column head in Table 2 in the version published ASAP November 14, 2006; the corrected version was published ASAP November 17, 2006.

SUPPORTING INFORMATION AVAILABLE

^{1}H, ^{13}C, and ^{31}P NMR spectra of the compounds produced during C_{32}phytBAS synthesis. This material is available free of charge via the Internet at http://pubs.acs.org.

REFERENCES

1. Langworthy, T. A. (1985) in *The Bacteria* (Woese, C. R., and Wolfe, R. S., Eds.) Vol. VIII, pp. 459-497, Academic Press, New York.
2. Damsté, J. S. S., Schouten, S., Hopmans, E. C., van Duin, A. C. T., and Geenevasen, J. A. J. (2002) Crenarchaeol: the characteristic core glycerol dibiphytanyl glycerol tetraether membrane lipid of cosmopolitan pelagic crenarchaeota, *J. Lipid Res. 43*, 1641−1651.
3. De Rosa, M., and Gambacorta, A. (1988) The lipids of archaebacteria, *Prog. Lipid Res. 27*, 153−175.
4. Kates, M. (1995) Adventures with membrane lipids, *Biochem. Soc. Trans. 23*, 697−709.
5. Patel, G. B., and Sprott, G. D. (1999) Archaeobacterial ether lipid liposomes (archaeosomes) as novel vaccine and drug delivery systems, *Crit. Rev. Biotech. 19*, 317−357.
6. Gräther, O., and Arigoni, D. (1995) Detection of regioisomeric macrocyclic tetraethers in the lipids of methanobacterium-thermoautotrophicum and other archaeal organisms, *Chem. Commun. 4*, 405−406.
7. Hopmans, E. C., Schouten, S., Pancost, R. D., van der Meer, M. T. J., and Damsté, J. S. S. (2000) Analysis of intact tetraether lipids in archaeal cell material and sediments by high performance liquid chromatography/atmospheric pressure chemical ionization mass spectrometry, *Rapid Commun. Mass Spectrom. 14*, 585−589.
8. Thompson, D. H., Wong, K., Humphry-Baker, R., Wheeler, J., Kim, J.-M., and Rananavare, S. B. (1992) Tetrather bolaform amphiphiles as models of archaebacterial membrane-lipids -Raman-spectroscopy, P-31 NMR, X-Ray scattering, and electron-microscopy, *J. Am. Chem. Soc. 114*, 9035−9042.
9. Elferink, M. G. L., de Wit, J. G., Driessen, A. J. M., and Konings, W. N. (1994) Stability and proton-permeability of liposomes composed of archaeal tetraether lipids, *Biochim. Biophys. Acta 1193*, 247−254.
10. Arakawa, K., Kano, H., Eguchi, T., Nishiyama, Y., and Kakinuma, K. (1999) Significance of the 72-membered macrocyclic structure found in archaeal membrane lipids: Model studies of the macrocyclic tetraether diphospholipids by calorimetric, P-31 NMR, and electron microscopic analyses, *Bull. Chem. Soc. Jpn. 72*, 1575−1581.
11. Arakawa, K., Eguchi, T., and Kakinuma, K. (2001) Highly thermostable liposome from 72-membered macrocyclic tetraether lipid: Importance of 72-membered lipid for archaea to thrive under hyperthermal environments, *Chem. Lett. 5*, 440−441.
12. Kim, J.-M., Patwardhan, A., Bott, A., and Thompson, D. H. (2003) Preparation and electrochemical behavior of gramicidin-bipolar

13. lipid monolayer membranes supported on gold electrodes, *Biochim. Biophys. Acta 1617*, 10−21.
13. Thompson, D. H., Patwardhan, A. P., Di M.eglio, C., Kim, J.-M., Haynes, R., Burden, D. L., and Rananavare, S. B., unpublished results.
14. Cornell, B. A., Braach-Maksvytis, V. L. B., King, L. G., Osman, P. D. J., Raguse, B., Wieczorek, L., and Pace, R. J. (1997) A biosensor that uses ion-channel switches, *Nature 387*, 580−583.
15. Wiess-Wichert, C., Smetazko, M., Valina-Saba, M., and Schalkhammer, T. (1997) A new analytical device based on gated ion channels: A peptide-channel biosensor, *J. Biomol. Screening 2*, 11−18.
16. Elferink, M. G. L., de Wit, J. G., Demel, R., Driessen, A. J. M., and Konings, W. N. (1992) Functional reconstitution of membrane-proteins in monolayer liposomes from bipolar lipids of Sulfolobus acidocaldarius, *J. Biol. Chem. 267*, 1375−1381.
17. In't Veld, G., Elferink, M. G. L., Driessen, A. J. M., and Konings, W. N. (1992) Reconstitution of the leucine transport-system of Lactococcus lactis into liposomes composed of membrane-spanning lipids from Sulfolobus acidocaldarius, *Biochemistry 31*, 12493−12499.
18. Romano, J. D., and Michaelis, S. (2001) Topological and mutational analysis of Saccharomyces cerevisiae Ste14p, founding member of the isoprenylcysteine carboxyl methyltransferase family, *Mol. Biol. Cell 12*, 1957−71.
19. Dai, Q., Choy, E., Chiu, V., Romano, J., Slivka, S. R., Steitz, S. A., Michaelis, S., and Philips, M. R. (1998) Mammalian prenyl-cysteine carboxyl methyltransferase is in the endoplasmic reticulum, *J. Biol. Chem. 273*, 15030−15034.
20. Anderson, J. L., Frase, H., Michaelis, S., and Hrycyna, C. A. (2005) Purification, functional reconstitution, and characterization of the Saccharomyces cerevisiae isoprenylcysteine carboxylmethyltransferase Ste14p, *J. Biol. Chem. 280*, 7336−7345.
21. Pillinger, M. H., Volker, C., Stock, J. B., Weissmann, G., and Philips, M. R. (1994) Characterization of a plasma membrane-associated prenylcysteine-directed alpha carboxyl methyltransferase in human neutrophils, *J. Biol. Chem. 269*, 1486−1492.
22. Stephenson, R. C., and Clarke, S. (1992) Characterization of a rat liver protein carboxyl methyltransferase involved in the maturation of proteins with the -CXXX C-terminal sequence motif, *J. Biol. Chem. 267*, 13314−13319.
23. Boivin, D., Gingras, D., and Beliveau, R. (1993) Purification and characterization of a membrane-bound protein carboxyl methyltransferase from rat kidney cortex, *J. Biol. Chem. 268*, 2610−2615.
24. Yoo, B. C., Kang, M. S., Kim, S., Lee, Y. S., Choi, S. Y., Ryu, C. K., Park, G. H., and Han, J. S. (1998) Partial purification of protein farnesyl cysteine carboxyl methyltransferase from bovine brain, *Exp. Mol. Med. 30*, 227−234.
25. Patwardhan, A. P., and Thompson, D. H. (1999) Efficient synthesis of 40-and 48-membered tetraether macrocyclic bisphosphocholines, *Org. Lett. 1*, 241−244.
26. Patwardhan, A. P., and Thompson, D. H. (2000) Novel flexible and rigid tetraether acyclic and macrocyclic bisphosphocholines: synthesis and monolayer properties, *Langmuir 16*, 10340−10350.
27. Peanasky, J., Schneider, H. M., Granick, S., and Kessel, C. R. (1995) Self-assembled monolayers on mica for experiments utilizing the surface forces apparatus, *Langmuir 11*, 953−962.
28. Groves, J. T., and Boxer, S. G. (1995) Electric field-induced concentration gradients in planar supported bilayers, *Biophys. J. 69*, 1972−1975.
29. Cremer, P. S., and Boxer, S. G. (1999) Formation and spreading of lipid bilayers on planar glass supports, *J. Phys. Chem. B 103*, 2554−2559.
30. Soumpasis, D. M. (1983) Theoretical-analysis of fluorescence photobleaching recovery experiments, *Biophys. J. 41*, 95−97.
31. Di Meglio, C., Rananavare, S., Svenson, S., and Thompson, D. H. (2000) Bolaamphiphilic phosphocholines: Structure and phase behavior in aqueous media, *Langmuir 16*, 128−133.
32. Schaffner, W., and Weissmann, C. (1973) Rapid, sensitive, and specific method for determination of protein in dilute-solution, *Anal. Biochem. 56*, 502−514.
33. Schreiber, S. L., Wang, Z., and Schulte, G. (1988) Group selective reduction of acetals related to the ansa chain of the streptovaricins −conformational and stereochemical analysis, *Tetrahedron Lett. 29*, 4085−4088.
34. Schwab, P., France, M. B., Ziller, J. W., and Grubbs, R. H. (1995) A series of well-defined metathesis catalysts−synthesis of [RuCl₂-

(=CHR')(PR₃)₂] and its reactions, *Angew. Chem., Int. Ed. Engl. 34*, 2039−2041.

35. Thompson, D. H., Svendsen, C. B., Di M.eglio, C., and Anderson, B. C. (1994) Synthesis of chiral diether and tetraether phospholipids−regiospecific ring-opening of epoxy alcohol intermediates derived from asymmetric epoxidation, *J. Org. Chem. 59*, 2945−2955.

36. Svenson, S., and Thompson, D. H. (1998) Facile and efficient synthesis of bolaamphiphilic tetraether phosphocholines, *J. Org. Chem. 63*, 7180−7182.

37. Febo-Ayala, W., Holland, D. P., Bradley, S. A., and Thompson, D. H. (2006) Lateral diffusion rate of an eicosanyl-based bisg-lycerophosphocholine in bolalipid membranes determined by PFG-NMR and FRAP, *Langmuir*, in press.

38. Lee, A. G. (2003) Lipid-protein interactions in biological membranes: a structural perspective, *Biochim. Biophys. Acta 1612*, 1−40.

39. Pilot, J. D., East, J. M., and Lee, A. G. (2001) Effects of phospholipid headgroup and phase on the activity of diacylglycerol kinase of Escherichia coli, *Biochemistry 40*, 14891−14897.

40. Cornelius, F. (2001) Modulation of Na, K-ATPase and Na-ATPase activity by phospholipids and cholesterol. I. Steady-state kinetics, *Biochemistry 40*, 8842−8851.

41. Killian, J. A. (1998) Hydrophobic mismatch between proteins and lipids in membranes, *Biochim. Biophys. Acta 1376*, 401−416.

42. Tyminski, P. N., Latimer, L. H., and O' Brien, D. F. (1985) Rhodopsin in polymerized bilayer-membranes, *J. Am. Chem. Soc. 107*, 7769−7760.

43. Tyminski, P. N., Latimer, L. H., and O' Brien, D. F. (1988) Reconstitution of rhodopsin and the cGMP cascade in polymerized bilayer-membranes, *Biochemistry 27*, 2696−2705.

44. Gibson, N. J., and Brown, M. F. (1993) Lipid headgroup and acyl chain composition modulate the MI-MII equilibrium of rhodopsin in recombinant membranes, *Biochemistry 32*, 2438−2454.

45. Yamauchi, K., Yamada, K., Kinoshita, M., and Kamikawa, T. (1991) Archaebacterial lipids−surface pressure-surface area isotherms of 1, 1'-(1, 32-dotriacontanediyl)bis[2-[3RS,7R,11R)-3,7,-11,15-tetramethyl-hexadecyl]sn-glycero-3-phosphocholine, *Bull. Chem. Soc. Jpn. 64*, 2088−2090.

46. Yamauchi, K., Sakamoto, Y., Moriya, A., Yamada, K., Hosokawa, T., Higuchi, T., and Kinoshita, M. (1990) Archaebacterial lipid models−highly thermostable membranes from 1,1'-(32-dotria-contamethylene)bis(2-phytanyl-sn-glycero-3-phosphocholine), *J. Am. Chem. Soc. 112*, 3188−3191.

47. Jarrell, H. C., Zukotynski, D. A., and Sprott, G. D. (1998) Lateral diffusion of the total polar lipids from Thermoplasma acidophilum in multilamellar liposomes, *Biochim. Biophys. Acta 1369*, 259−266.

BI061159C